

```

S5a          MVLESTMVCVDNSEYMRNGDFLPTRLQAQQDAVNI VCHSKTRS NPENNVGLITLANDCEV 60
Angiocidin  MVLESTMVCVDNSEYMRNGDFLPTRLQAQQDAVNI VCHSKTRS NPENNVGLITLANDCEV 60
*****

S5a          LTTLTPTDGRILSKLHTVQPKGKITFCTGIRVAHLAL KHRQGKNHKMRI IAFVGS PVEDN 120
Angiocidin  LTTLTPTDGRILSKLHTVQPKGKITFCTGIRVAHLAL KHRQGKNHKMRI IAFVGS PVEDN 120
*****

S5a          EKDLVKLAKRLKKEKVNVDI INFGE EEVNTEKLTAFVNTLNGK DGTGSHLVTVP GP PSLA 180
Angiocidin  EKDLVKLAKRLKKEKVNVDI INFGE EEVNTEKLTAFVNTLNGK DGTGSHLVTVP GP PSLA 180
*****

S5a          DALISSPILAGEGGAMLGLGASDFEFGVDPSADPELALALRVSMEEQRQRQEEEEARRAAA 240
Angiocidin  DALISSPILAGEGGAMLGLGASDFEFGVDPSADPELALALRVSMEEQRQRQEEEEARRAAA 240
*****

S5a          ASAAEAGIATTGTE---DSDDALLKMTISQQEFGRTGLPDLSSMTEEEQIAYAMQMSLQG 297
Angiocidin  ASAAEAGIATTGTEGERDSDDALLKMTISQQEFGRTGLPDLSSMTEEEQIAYAMQMSLQG 300
*****

S5a          AEFGQAESADIDASSAMDTSEPAKEEDDYDVMQDPEFLQSVLENLPGVDPNNEAIRNAMG 357
Angiocidin  AEFGQAESADIDASSAMDTSEPAKEEDDYDVXQDPEFLQSVLENLPGVDPNNEAIRNAMG 360
*****

S5a          SLASQATKDGKDKKKEEDKK 377
Angiocidin  SLASQATKDGKDKKKEEDKK 380
*****

```

**Fig. S1. The BLAST result of S5a and Angiocidin.** A BLAST run was done using NCBI within the NR database using S5a as the query to identify proteins that are similar to Angiocidin.

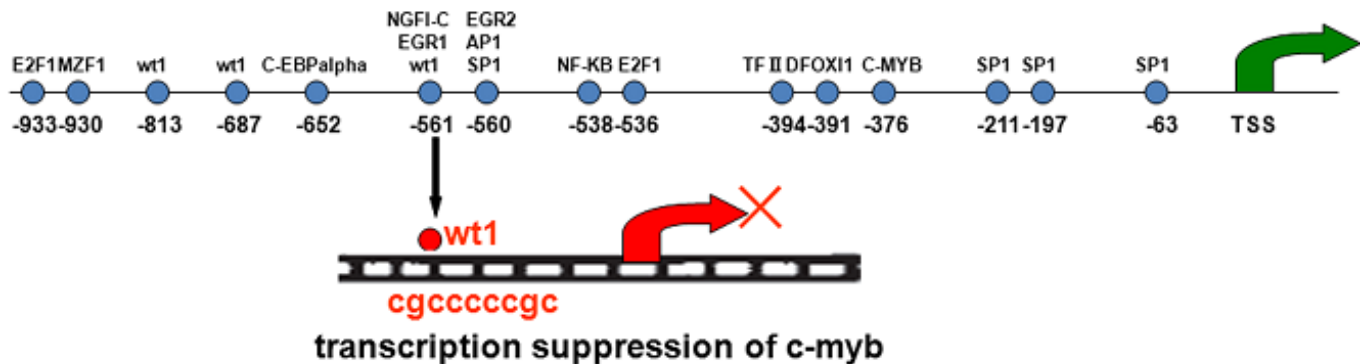


**Fig. S2. Bioinformatics analysis of WT1 and c-myb.** We put the sequence mapped from -1000 bp to TSS (transcription start site) into TESS database, and obtained various transcription factors which can interact with the above sequence. After that, we chose some transcription factors (La value  $\geq 16$ ) as important research targets, because they have stronger affinity with target sites than other transcription factors. Among these molecules, WT1 transcription factor can bind the sequence 5'cgcccccg' on the c-myb promoter.

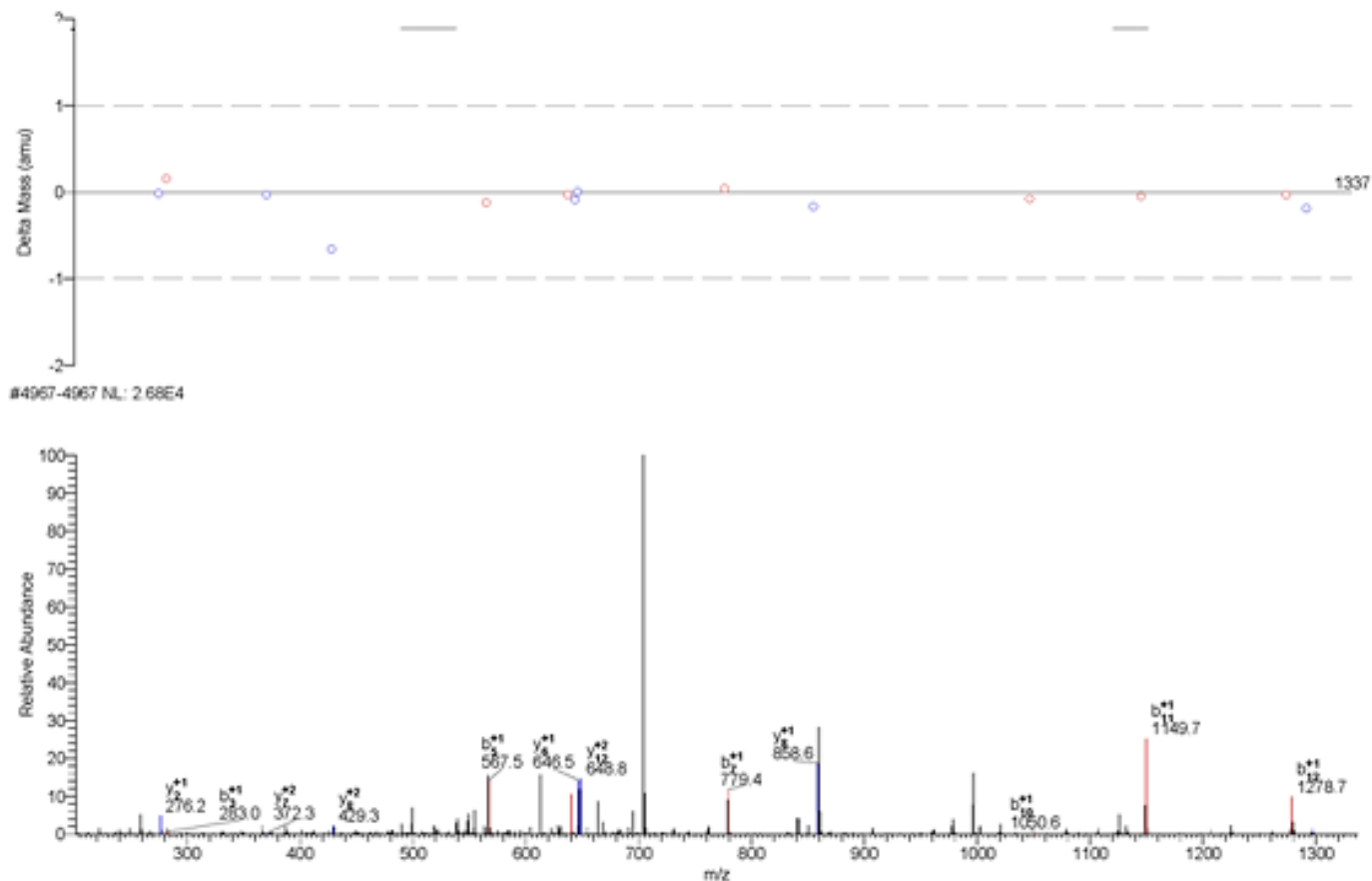


**Fig. S3. Detection of DR6 peptide fragment by MS.** The extracted peptides from the gel piece were sent to Shanghai Applied Protein Technology Co. Ltd for analysis and identification. A detailed description of each of these steps follows. The Ettan™ MDLC system (GE Healthcare) was applied for desalting and separation of tryptic peptide mixtures. In this system, samples were desalted on RP trap columns (Zorbax 300SB-C18, Agilent Technologies) and separated on a RP column (150  $\mu$ m i.d., 100 mm length, Column Technology Inc., Fremont, CA). The mobile phase A (0.1% formic acid in HPLC-grade water) and the mobile phase B (0.1% formic acid in acetonitrile) were selected. Tryptic peptide mixtures (20  $\mu$ g) were loaded onto the columns, and separation was performed at a flow rate of 2  $\mu$ L/min by using a linear gradient of 4–50% B for 120 min. A Finnigan™ LTQ™ linear ion trap MS (Thermo Electron) equipped with an electrospray interface was connected to the LC setup for detection of eluted peptides. Data-dependent MS/MS spectra were obtained simultaneously, and each scan cycle consisted of one full MS scan in profile mode followed by five MS/MS scans in centroid mode with the following Dynamic Exclusion™ settings: repeat count 2, repeat duration 30 s, exclusion duration 90 s. Each sample was analyzed in triplicate. MS/MS spectra were automatically searched against the non-redundant International Protein Index (IPI) human protein database (version 3.26, 67687 entries) using the Bioworks Browser rev. 3.1. The peptides were constrained to be tryptic, and up to two missed cleavages were allowed. Carbamidomethylation of cysteines were treated as a fixed modification whereas the oxidation of methionine residues was considered to be a variable modification. The mass tolerance allowed for the precursor ions was 2.0 Da and for fragment ions, this value was 0.0 Da. The protein identification criteria were based on Delta CN ( $\geq 0.1$ ) and cross-correlation scores (Xcorr, one charge  $\geq 1.9$ , two charges  $\geq 2.2$ , three charges  $\geq 3.75$ ).

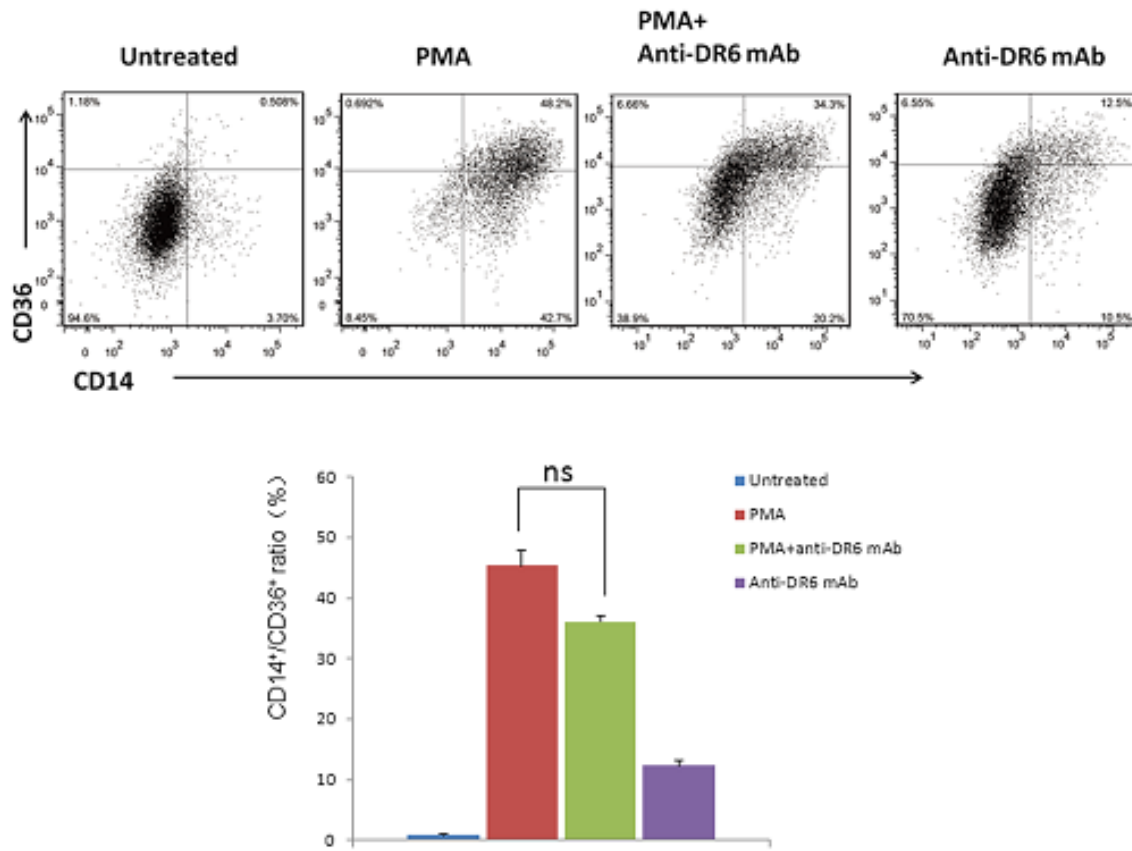


**Fig. S4. Anti-DR6 antibody have no effect on THP-1 differentiation induced by PMA.** Flow cytometry check were performed on THP-1 cells at 72 h after DR6 antibody treatment, which have no effect on differentiation induced by PMA (100 ng/mL). The experiment was repeated thrice, and the data presented represent a typical experiment. The results from combined analyses are shown (mean±s.d.,  $n=3$ ).

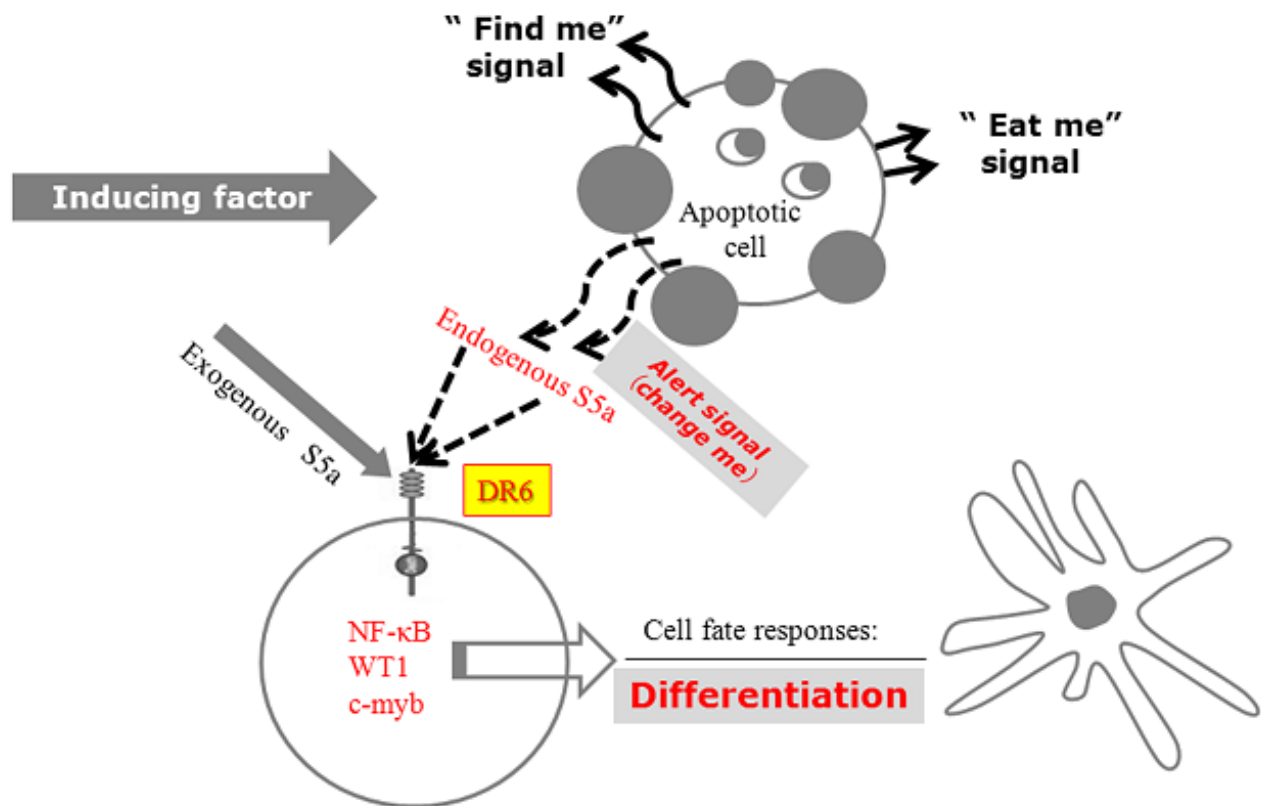


**Fig. S5. The differentiation-inducing effects and interaction mechanism between S5a and DR6 on THP-1 cells.** Apoptotic THP-1 cells released S5a, which was recognized by DR6 on the surface of neighboring cells. In the tumor microenvironment, the signals could alert neighboring cells to escape the lethal effects of the inducing factor, thereby modulating their state of differentiation and influencing the consecutive immune responses.

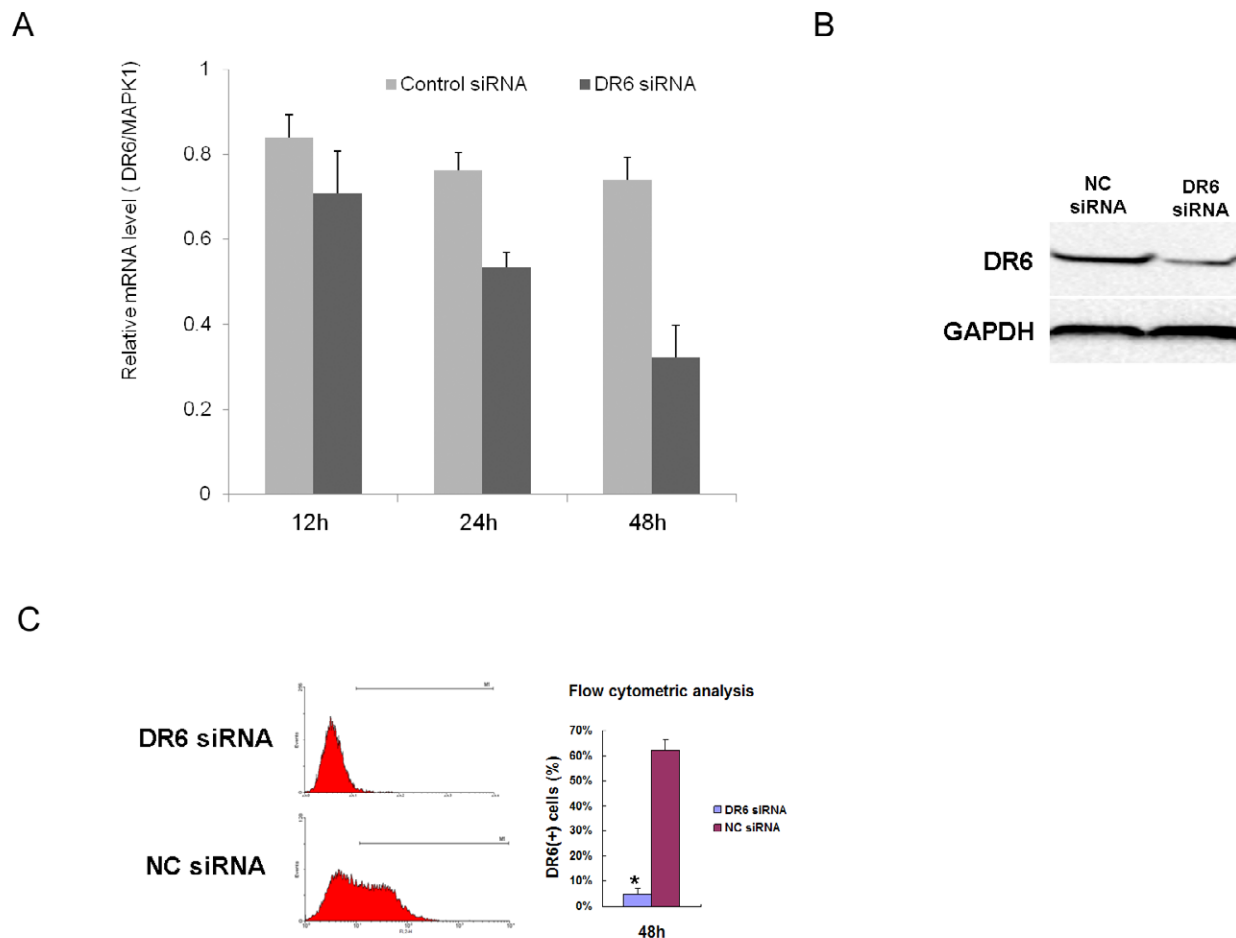


**Fig. S6. Knockdown the expression of DR6 in THP-1 cells.** THP-1 cells were transfected with DR6 siRNA or Scrambled siRNA (Control) using HiPerFect Transfection Reagent (QIAGEN). (A) Knockdown of intracellular DR6 by siRNA was confirmed by quantitative, real-time RT-PCR. (B) Western blot analysis of intracellular DR6 knockdown effect after DR6 siRNA treatment for 48 h. (C) Flow cytometric analysis confirmed that the expression of DR6 significantly decreased on the cell surface of THP-1 after siRNA treatment for 48 h (\* $P < 0.05$ ).

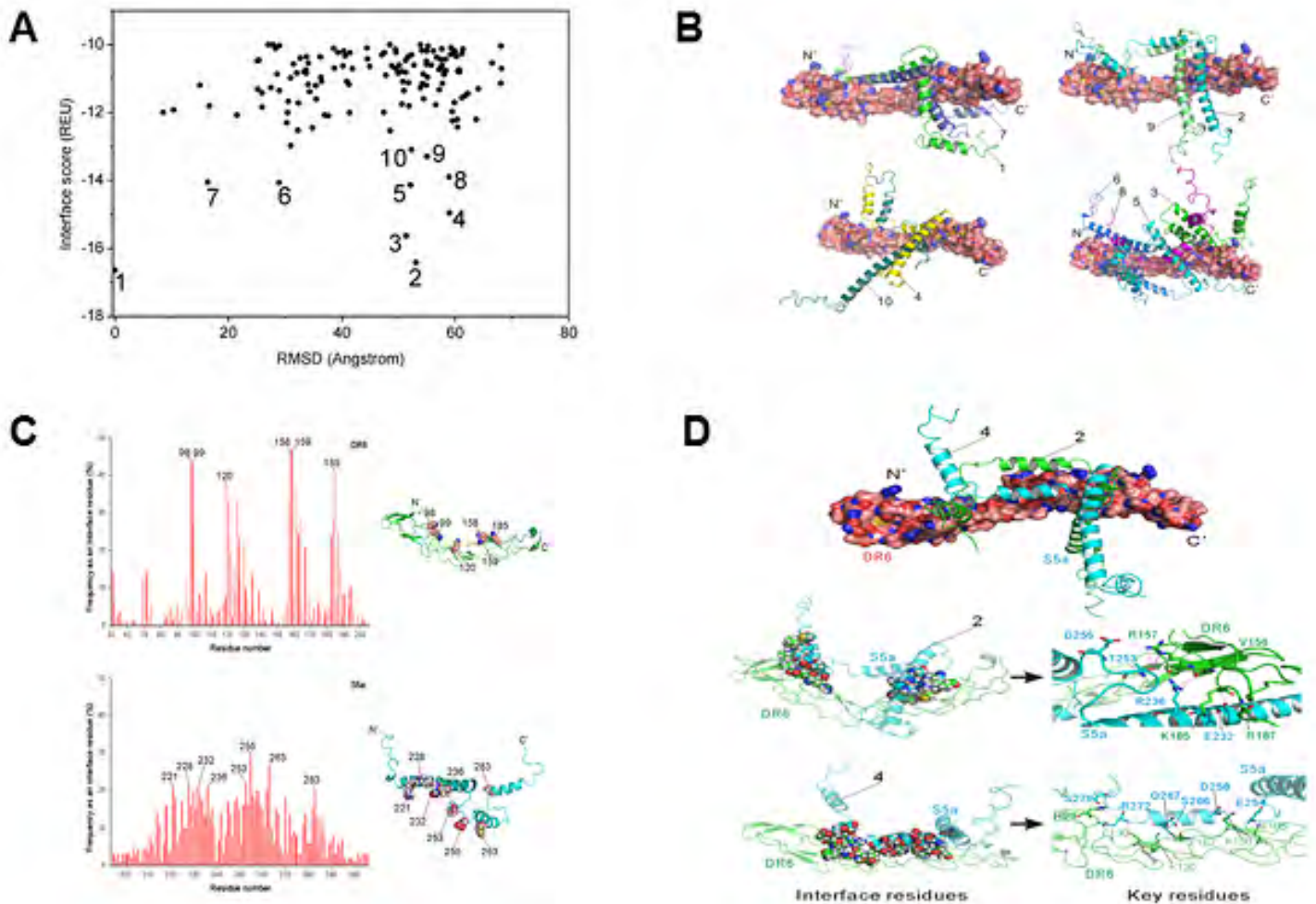


**Fig. S7. Computational prediction and analysis of the DR6-S5a interaction.** Using Rosetta Docking to obtain 20,000 docking structures of DR6 and S5a, and then analyzed by the InterfaceAnalyzer module in Rosetta. These structures were then ranked by their interface energies. The selection criteria are: the interface energy  $\leq -10$  REU (Rosetta energy unit), the number of unsatisfied hydrogen bonds  $< 10$ , packing statistic score for the interface  $> 0.60$ . (A) The RMSD-interface energy plot of the 143 lowest-energy conformations. Each dot represents one docking conformation. The lowest-energy conformation is the reference for the RMSD calculations. (B) The 10 lowest interface energy conformations of DR6 and S5a. DR6 is illustrated by surface model, and S5a by cartoon model. Conformation 1 is the lowest-energy complex. To judge by the orientation of S5a, conformations 2, 4, 9 and 10 are quite similar. Since these are 40% of the 10 lowest-energy conformations, it is likely that S5a binds to DR6 using the same orientation in conformations 2, 4, 9 and 10. Based on the 143 lowest-energy conformations, we also calculate the frequencies of protein residues as interface residues, in order to reveal the most probable interface residues (i.e. the more the frequency is, the more probable the residue as an interface residue). (When the distance between any atom of a residue of DR6 (S5a) to any atom of S5a (DR6) is less than  $3.0 \text{ \AA}$ , we defined the residue as an interface residue). (C) The most probable interface residues deduced from the 143 lowest-energy conformations. (D) Two representative binding conformations of DR6-S5a, considering by the interface energy and the most probable interface residues.

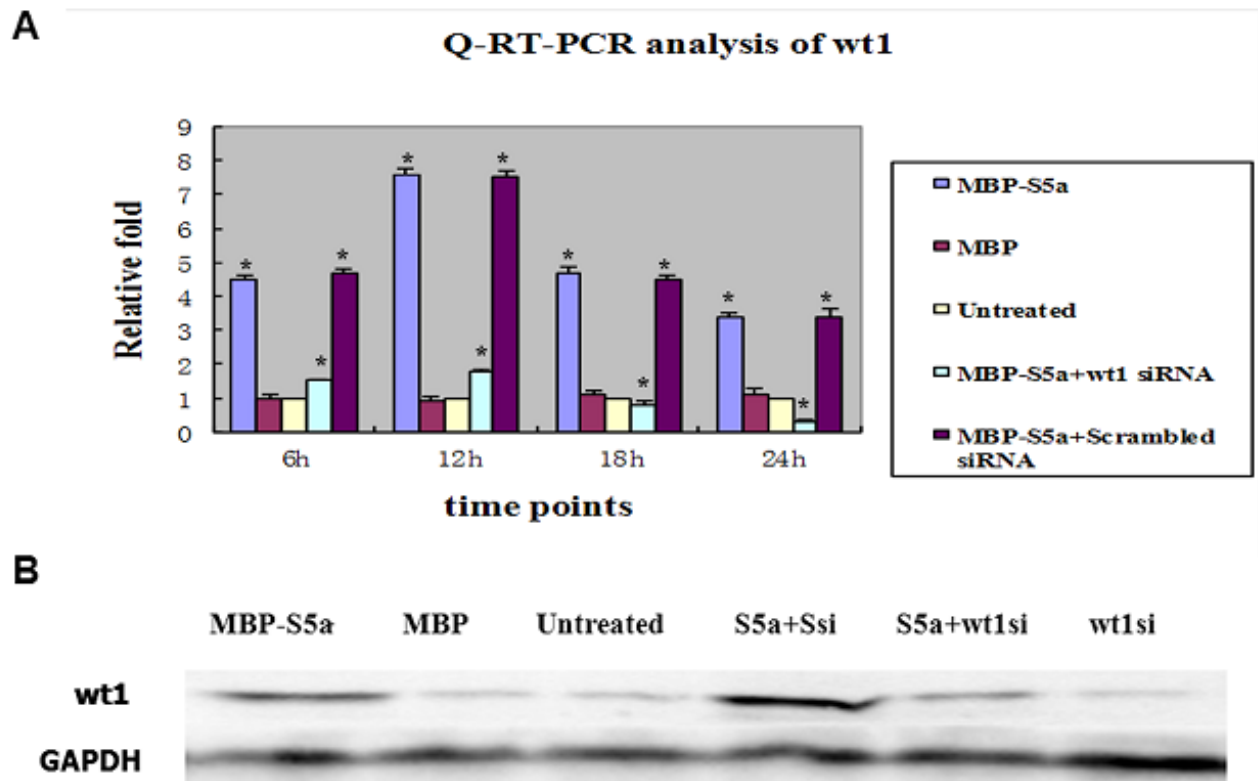


**Fig. S8. The upregulation of WT1 was successfully blocked by siRNA even if cells were treated with S5a.** (A) We used *WT1* siRNA to pretreat THP-1 cells for 8 h, then we treated cells with S5a to observe the expression of WT1, only MBP-S5a, only MBP, and untreated groups were parallel groups. After treating cells with S5a, we extracted the RNA at different time points (6 h, 12 h, 18 h, 24 h) to analyze the expression of WT1 by Q-RT-PCR, the results indicated that the upregulation of WT1 was successfully blocked by siRNA even if cells were treated with S5a ( $*P < 0.05$ ). (B) The result of western-blot analysis was consistent with the Q-RT-PCR results.